POLITECNICO
MILANO 1863

SCUOLA DI INGEGNERIA INDUSTRIALE
E DELL'INFORMAZIONE

EXECUTIVE SUMMARY OF THE THESIS

BFDS-MOMEDA-LIA: Deconvolution in Bounded Finite Dimensional Space for Early Fault Diagnosis of Rotating Machinery

TESI MAGISTRALE IN MOBILITY ENGINEERING – INGEGNERIA MOBILITY

AUTHOR: MENG ZHANG

ADVISOR: ALESSANDRO FERRERO

ACADEMIC YEAR: 2023-2024

1. Introduction

Rolling bearings provide reliable and stable support for rotating machinery, and their operational condition significantly impacts the performance of mechanical systems. Operating in harsh environments such as heavy loads and high temperatures for extended periods makes key components of bearings susceptible to damage, typically manifested as surface damage to major elements (outer ring, inner ring, cage, or rolling elements) [1]. These unexpected failures can lead to unplanned downtime or even catastrophic harm to personnel [2]. Therefore, early identification of the type of failure and assessment of the fault severity are of paramount importance.

Over the past few decades, vibration-based techniques for extracting fault features in rotating machinery have undergone in-depth research, leading to the development of a variety of technologies. These include spectral kurtosis [3], cyclostationary methods [4], decomposition-based approaches [5], morphological filtering [6], stochastic resonance [7], blind source separation [8], and machine learning methods [9]. Identifying early-stage faults from vibration signals can be challenging because the impulse patterns caused by faults are often masked by background noise and other interferences. The situation is further complicated by the propagation effects of unknown transmission paths [10]. Therefore, effectively extracting subtle fault information from vibration signals is crucial for accurate fault diagnosis.

Each time rotating components pass through a faulty area, pulses are generated in the measured signal. Therefore, a series of sparse pulses are considered a crucial indicator of mechanical faults in rotating machinery [11]. When the speed is constant, these sparse pulses caused by faults in rotating components, such as bearing or gear faults, exhibit distinct periodicity or cyclostationarity [1]. Lock-in amplifiers (LIA) have been widely used to measure weak periodic signals in the presence of noise [12, 13]. This system employs a technique called phase-sensitive detection, allowing the detection of the amplitude of input signal components at the frequency of a reference signal.

Once the reference signal is modulated to the characteristic frequency of a bearing fault, for instance, LIA can be utilized to estimate the amplitude of signal components at that characteristic frequency.

Gaining precise values for these characteristic frequencies has become a critical challenge, as it directly determines whether the measurement function of the LIA can be accurately implemented. If the LIA adopts incorrect characteristic frequencies from the outset, the measured results may not effectively reflect the pulse signals triggered by faults [14]. Generally, the theoretical fault characteristic frequencies of rolling bearings can be calculated based on the geometric relationships of the bearings [1]. However, due to the presence of assembly tolerances, manufacturing errors, and speed fluctuations, the actual characteristic frequencies often deviate from the calculated values [15].

In order to provide guidance on fault frequency for LIA, this study proposes to use Blind Deconvolution (BD) to highlight the periodic pulse components in the signal to obtain a reliable fault frequency for LIA to measure. Blind deconvolution [16, 17] aims to design an optimal inverse filter to recover (deconvolve) the input signal from a noisy observed signal. BD holds unique advantages in bearing fault diagnosis, because the transmission process of the fault source signal in rolling bearing faults involves the convolution mixture of the source signal with noise, while BD can extract fault impulses by designing a filter [18, 19]. Currently, representatives of the BD methods in bearing fault diagnosis are the Minimum Entropy Deconvolution (MED) [20], Maximum Correlated Kurtosis Deconvolution (MCKD) [21] and Multi-point Optimal Minimum Entropy Deconvolution Adjusted (MOMEDA) [22].

This work initially introduces a novel deconvolution method based on the Multi D-norm, termed Blind Deconvolution with Bounded Finite-Dimensional Space Optimization (BFDS-MOMEDA), to highlight the periodical impulses caused by bearing fault. This method overcomes the convergence challenges of filter coefficients in the "optimization-deconvolution" approach used in prior works. Additionally, a fault diagnosis framework has been proposed, termed BFDS-MOMEDA-LIA, where blind deconvolution guides the lock-in amplifier in the fault diagnosis process. The reference frequency for the LIA is provided by blind deconvolution, avoiding the issue of inaccuracies in estimating reference frequencies based on geometric relationships. The proposed approach is validated using both simulated and experimental data from bearing tests. Simulation and experimental results demonstrate that the proposed framework effectively diagnoses bearing faults through vibration signals, showing the superior compared with previous work.

BFDS-MOMEDA-LIA method uses the unique advantages of the two methods, complements the potential defects, and comprehensively realizes the extraction and quantification of early weak fault information. In order to confirm the validity of the proposed framework from a metrological perspective, the uncertainty in the measurement process from JCGM 100 [23] and JCGM 101 [24] perspectives has been discussed. This study quantifies the uncertainty in the diagnosis process, and provides guidance for future potential work.

2. Method

2.1. BFDS-MOMEDA

Reference [25-26] proposed an optimization-deconvolution method, and it has been proven to be a very practical way to employ optimization algorithm to solve the deconvolution issue. In [x], the authors suggest an optimization space termed generalized hypersphere domain, aiming to avoid the redundancy of optimization searching.

It is acknowledged that [25-26] presented a feasible way to achieve optimization-deconvolution method. However, this study has proved that method in [25-26] has an unavoidable problem: the designed filter always converges with the increasing of filter length.

The consequence is that it is always almost not possible to design a long filter, which indicates a waste on filter resources. This short-coming make the method in [25-26] unsuitable for scenarios that required a relatively long filter.

To address these issues, this study proposed a new optimization approach that involves a bounded and finite-dimensional optimization space (BFDS). For an inverse filter of length L, a dimensional orthogonal space is defined with upper and lower bounds [b_n, u_n] in the nth dimension.

Thus, the constructed L-dimensional optimization space is BFDS, as shown in Figure. 1.

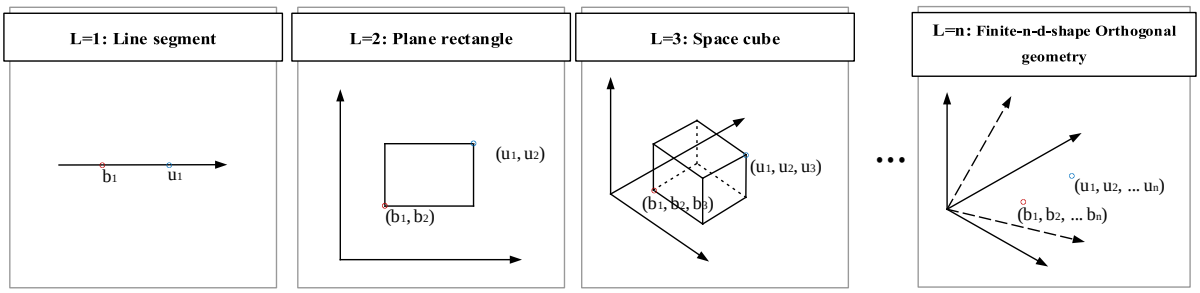

Fig. 1. Bounded Finite-Dimensional Orthogonal Space (BFDS).

Once the optimization space is determined, the optimization-deconvolution problem has become the problem of finding a best position in BFDS, where its coordinate in n^{th} dimension represents n^{th} filter coefficient value. Here, the "best position" refers to the position that minimalized the norm in relative benchmark deconvolution method. Since the MOMEDA has been selected as the benchmark, the norm refers to the multi D-norm [22]:

$$K_{MOMEDA}(\boldsymbol{f}) = \max_{k=1,2,\ldots,N} \frac{1}{\|\boldsymbol{t}\|} \frac{\boldsymbol{t}^T \boldsymbol{y}}{\|\boldsymbol{y}\|}. \quad (1)$$

In the equation, $\boldsymbol{t}$ is a constant vector indicating the positions of the pulses, y is the fault signal recovered, $\boldsymbol{f}$ is the designed filter.

For example, in a signal of length N, indicating the positions of pulses at the n_1, n_2, ..., n_m sampling positions, with a total of m pulses, it can be expressed as:

$$\boldsymbol{f}_{opt,MOMEDA} = \{\boldsymbol{f}_{opt,MOMEDA}: K_{MOMEDA}(\boldsymbol{f}_{opt,MOMEDA}) > K_{MOMEDA}(\boldsymbol{f}), \forall \boldsymbol{f} \in \Re^L\} \quad (2)$$

L is the length of filter. If the autocorrelation matrix $\boldsymbol{X}_0\boldsymbol{X}_0^T$ is invertible, then the process of iteratively solving the inverse filter is:

$$\boldsymbol{X}_0 = \begin{bmatrix} x_L & x_{L+1} & \cdots & x_N \\ x_{L-1} & x_L & \cdots & x_{N-1} \\ \vdots & \vdots & \ddots & \vdots \\ x_1 & x_2 & \cdots & x_{N-L+1} \end{bmatrix}_{L\times(N-L+1)} \quad (3)$$

The fault signal recovered is:

$$\boldsymbol{y} = \boldsymbol{X}_0^T \boldsymbol{f}_{opt,MOMEDA}. \quad (4)$$

2.2. Lock-in amplifier (LIA)

The purpose of the LIA is to estimate the amplitude and phase of a periodic signal disrupted by noise at a frequency determined by a reference signal. Under the theoretical condition that the measurement signal is uncorrelated with noise, the LIA employs phase-sensitive detection to detect spectral components of the input signal at the so-called reference signal frequency. It multiplies the measured target signal with a reference signal of known frequency to achieve frequency shifting. Subsequently, a low-pass filter is used to eliminate noise and high-frequency components, obtaining a DC component with a fixed mathematical relationship to the amplitude of the detected low signal-to-noise ratio signal.

The common LIA architecture used for weak signal detection is the orthogonal vector lock-in amplifier. Two reference signals, with the same frequency and a phase difference of 90 degrees, are employed along with the target signal (a sinusoidal signal mixed with noise at multiple magnitude levels). The output of the LIA's later stage comprises two DC signals, $\boldsymbol{I}$ and $\boldsymbol{Q}$, which contain both the amplitude and phase information of the measured signal.

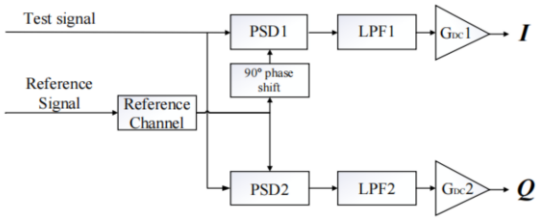

Fig. 2. Orthogonal vector type lock-in amplifier's common scheme.

2.3. Diagnosis framework

The signal extracted through the BFDS-MOMEDA process undergoes filtering, leading to the loss of original information. The waveform of the pulse signal is distorted because the extracted signal can only observe the pulses' peak positions, failing to display the waveform characteristics of the original pulse signal. The pulse signal experiences uncontrollable distortion. While a simple BD method can provide evidence for the presence or absence of fault pulses, it is essential to evaluate the strength characteristics of the fault signal

components by revisiting the original measured signal based on the extracted periodicity.

This study proposes a bearing fault diagnosis framework based on vibration signals, as illustrated in the Figure. 3 below:

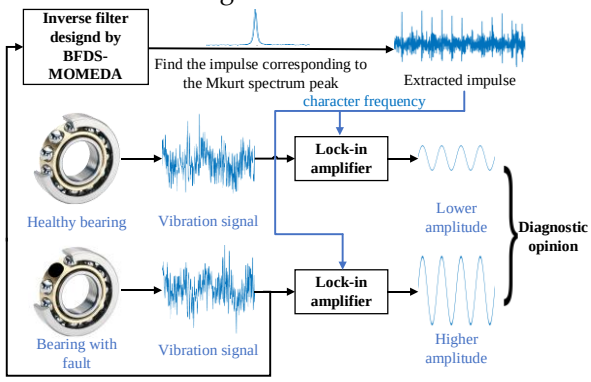

Fig. 3. BFDS-MOMEDA-LIA architecture.

In this framework, the vibration signals collected from the bearing under diagnosis first undergo the BD process. The identification of the pulse period is achieved by following [22]'s recommendation, using the MOMEDA MKurt spectrum to locate peaks and thereby preliminarily extract fault pulses. Specifically, when dealing with signals where the specific value of the fault period is unknown, BFDS-MOMEDA incrementally solves the MOMEDA MKurt spectrum in frequency intervals (often near the theoretical fault frequency, although we do not assume it accurately reflects the fault). When a frequency is found where the MKurt spectrum reaches its maximum value, the extracted pulse signal at that frequency is taken as the result of BD and serves as a guide for the reference frequency of the LIA. The LIA measures the original vibration signal directly according to the guided frequency, obtaining the amplitude of the signal component at the reference frequency in the original signal. By comparing the obtained results with a baseline bearing, bearing fault diagnosis is achieved.

The key idea of BFDS-MOMEDA-LIA framework is that if the LIA uses wrong fault frequency to measure the magnitude, the result is always wrong. This framework use frequency calculated by BD rather than simply use geometric formula [1], which has been proven to be easily influenced by various factors in real-world scenarios.

2.4. Uncertainty assessment

The principle of BFDS-MOMEDA-LIA is, on the fault frequency calculated by BFDS-MOMEDA, LIA's measured level is higher when fault occurs. To compare the measurement results of both suspicious and healthy bearings, it is required to represent measurement results with uncertainty. Otherwise, the measured results are meaningless in the metrological perspective.

The "Guide to the Expression of Uncertainty in Measurement" (GUM) [23] defines **measurement uncertainty** as "*parameter, associated with the result of a measurement, that characterizes the dispersion of the values that could reasonably be attributed to the measurand*". The word uncertainty means doubt, and thus in its broadest sense "**uncertainty (of measurement)**" means doubt about the validity of the result of a measurement.

Uncertainty of measurement is thus an expression of the fact that for a given measurand and a given result of measurement of it, there is not one value but an infinite number of values dispersed about the result that are consistent with all the observations and data and one's knowledge of the physical world, and that with varying degrees of credibility can be attributed to the measurand. [23]

In that case, to prove the measurement result on suspicious bearing in higher than that on healthy bearing, the measurement results must have character described in following Figure. 4:

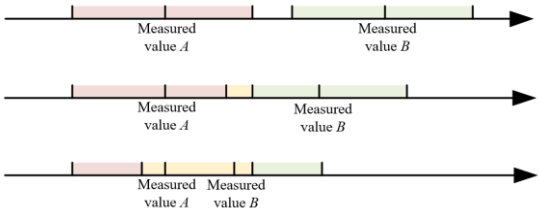

Fig. 4. In the first case only, the measurement results can be considered "separate".

To evaluate the uncertainty of proposed framework, two methodology roadmaps has been given:

1. In GUM, it is suggested that the components of measurement uncertainty should be grouped into two categories, **Type A** and **Type B**, according to whether they were evaluated by statistical methods or otherwise. Type A evaluation, described in VIM [27] as "*evaluation of a component of measurement uncertainty by a statistical analysis of measured*

quantity values obtained under defined measurement conditions", is firstly employed for characterize the measurement process of BFDS-MOMEDA-LIA.

2. GUM has provided detailed description of **Monte Carlo Methods (MCM)** on uncertainty within JCGM 101 Supplement [24]. The propagation of distributions implemented using MCM can validly be applied, and the required summary information subsequently determined, using the approach provided in this Supplement, under the certain conditions.

3. Results and discussion

3.1. Superior of BFDS-MOMEDA

In order to compare different deconvolution methods, a simulation signal as shown in the figure below is first constructed. In the absence of special instructions, the input signals used in the different methods in this chapter are the "superposed signal " in the Figure. 5 below.

Here, (a) is the periodic pulse train signal component, (b) is the random pulse component, (c) is the harmonic interference component, (d) is the white noise, and (e) is the superposed signal, which is simulated as the measured signal.

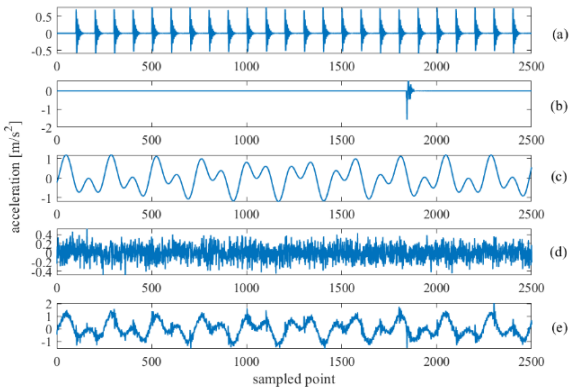

Fig. 5. Simulated signal in time-domain.

Filters of lengths 25, 50, 100, and 200 were designed using both the approach in [25] and the BFDS-MOMEDA method (Particle swarm optimization, PSO has been employed as the optimization method).

It is important to emphasize again that BFDS is not an optimization method, it only provides an optimization space for "optimization-deconvolution" problems. In the context of the proposed problem, it provides an upper and lower bound for each coefficient on the filter, thereby narrowing the scope of the optimization and avoiding the problem of the optimization falling into non-convergence.

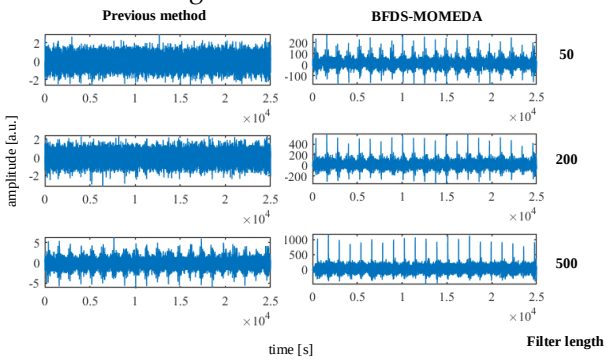

Fig. 6. Comparison of the processed signals with two methods.

In Figure. 6, it is evident that with an increase in filter length, the BFDS-MOMEDA method consistently and effectively extracts the pulse features from the signal, and as the filter length increases, the features become more pronounced. In contrast, the method in the generalized spherical optimization space struggles to efficiently extract pulse features. It is only when the filter length reaches 500 that the method in the generalized spherical optimization space can roughly discern the waveform of the pulse from the time-domain signal. However, this performance is even inferior to the results achieved by the BFDS-MOMEDA method with a filter length as short as 50.

The main reason behind this phenomenon lies on the different designed filters:

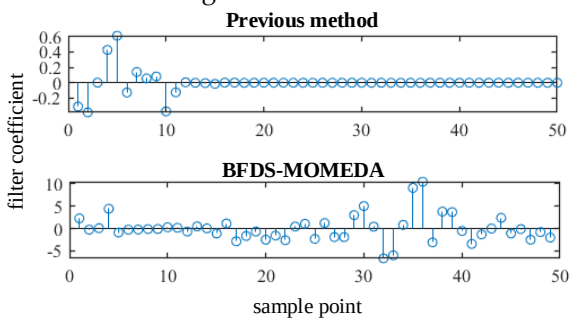

Fig. 7. Comparison of filters designed by two methods.

It can be observed that BFDS-MOMEDA has more flexibility in the shape of filter, without the constrains of filter length, thus achieving better performance with shorter filter.

This precisely validates the effectiveness of the BFDS-MOMEDA method. With a given length of filter resources, it achieves a more efficient design

of filter coefficients. Moreover, it demonstrates superior performance in applications with long fault periods and high sampling rates, tending to achieve better results with shorter filters.

3.2. Experiment on MFPG dataset

The Mechanical Failures Prevention Group (MFPG) provides a bearing failure data set for testing diagnostic and predictive algorithms [28].
The experimental data included three sets of healthy bearings and three sets of faulty outer ring bearings. Except the bearing itself, all the external conditions of the included experimental data collection were consistent. Firstly, the signals is processed by BFDS-MOMEDA, aiming to highlight the periodic impulse component:

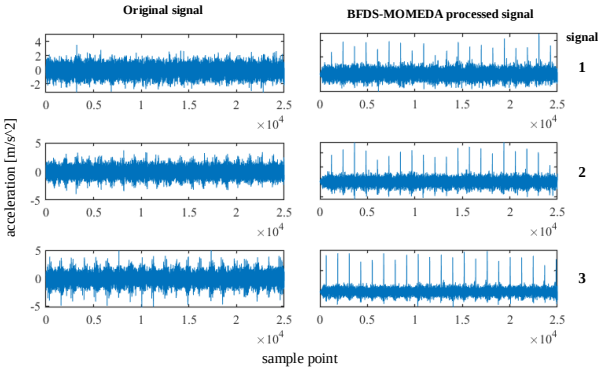

Fig. 8. Comparison of the original signals with the processed signals.

It is evident that for all 3 bearing, BFDS-MOMEDA has successfully extracted the impulse component. Frequency of these component can be then considered as reference frequency of LIA.
Taking the first group of faulty bearings as an example, it can be preliminarily observed that the LIA output level of suspicious bearings is separated from that of healthy bearings.

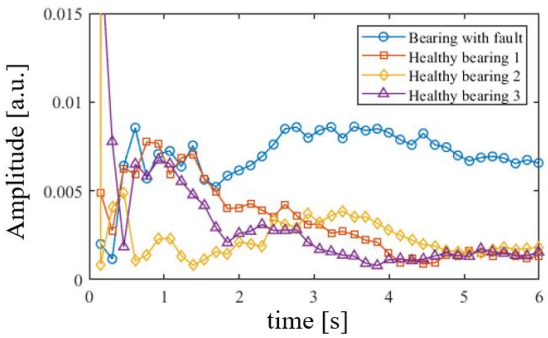

Fig. 9. Comparison of LIA outputs on suspicious and healthy bearings.

3.3. Uncertainty assessment

Measurement result is *set of quantity values being attributed to a measurand together with any other available relevant information*. If the measurement uncertainty is considered not to be negligible, a complete measurement can never be represented by a single measured quantity value. Although the LIA output on the suspect bearing in 3.2 has been observed with a preliminary separation compared to the healthy bearing, it is necessary to assess the uncertainty to ensure this separation.
A simulated Type A evaluation was used for the initial assessment. By adding a normal distribution of noise to the original data, the experimental session simulated the results of 10 measurements on the bearing in one minute.
In this case, arithmetic mean of 10 observations is calculated as $6.552 \cdot 10^{-3}$, and Type A standard uncertainty is $2.48 \cdot 10^{-4}$.
With the Guidance in JCGM 101 Supplement, MCM approach serves as the subsequent uncertainty assessment. After 5000 MCM samples with superposed normal distributed noise, LIA's output is fitted with normal distribution:

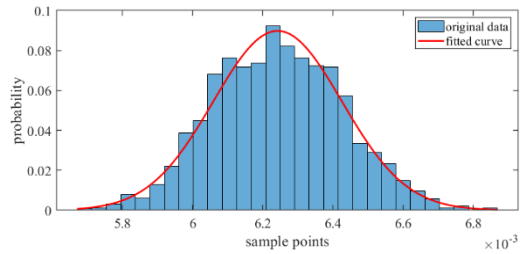

Fig. 10. The data obtained by the MCM method are used to fit the distribution.

In cases where the probability distribution has been obtained, the measurement uncertainty of interest at different confidence levels can always be obtained via probability density:

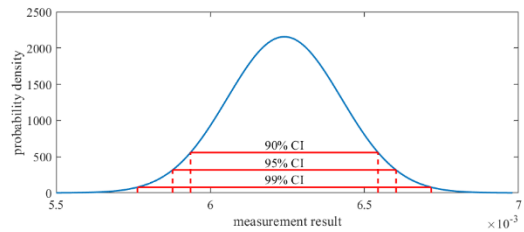

Fig. 11. Uncertainty under different confidence levels.

In this case, with 95% confidence, the expanded uncertainty is $3.59 \cdot 10^{-4}$ m/s².

It should be noted that there is reason to believe that continuing to increase the number of experiments appropriately would potentially enhance the reliability of the results, although this would also entail greater computing power consumption.

Where PDF is known, measurements with uncertainty can be characterized on the raw data to see if the measurement results on the abnormal bearing are separate from the measurement results on the healthy bearing:

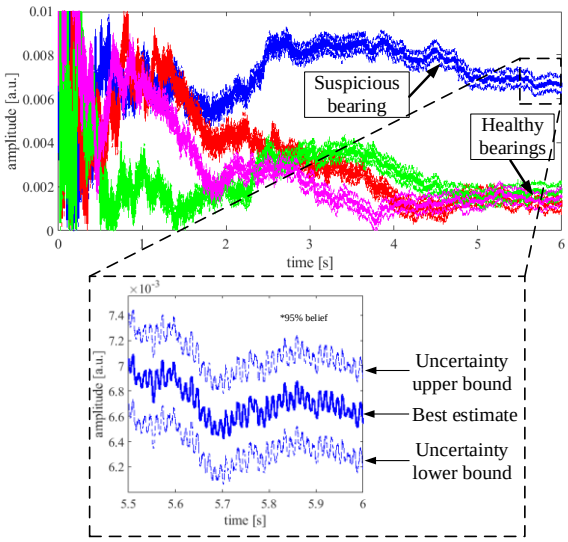

Fig. 12. The measurement results with uncertainty, comparison between the suspicious bearing and three healthy bearings.

As can be seen, at 95% confidence, there is a significant difference between the measurement results on the suspicious bearing and the measurement results on the healthy bearing. This difference is characterized from a metrological point of view, which further confirms that the method proposed in this study can effectively distinguish faulty bearings from healthy bearings, and thus achieve fault detection.

4. Conclusion

A framework, BFDS-MOMEDA-LIA, is developed for early fault detection in rolling machinery in this work. It employs blind deconvolution and heuristic optimization to highlight fault features, overcoming previous convergence issues. Integrating lock-in amplifier (LIA) and blind deconvolution (BD) approaches, it balances fault extraction and waveform preservation. BD captures fault features while damaging original waveform, while LIA accurately measures fault amplitude but is frequency-sensitive. BFDS-MOMEDA-LIA combines both advantages, enhancing fault detection in time and frequency domains. Experimental results on open datasets validate its effectiveness, sensitivity, and industrial value. Using GUM-guided analysis and Monte Carlo simulation, measurement uncertainty in fault detection is assessed, affirming its metrological capability.

Bibliography

[1] Randall, R. B., & Antoni, J. (2011). Rolling element bearing diagnostics—A tutorial. Mechanical systems and signal processing, 25(2), 485-520.

[2] Vrignat, P., Kratz, F., & Avila, M. (2022). Sustainable manufacturing, maintenance policies, prognostics and health management: A literature review. Reliability Engineering & System Safety, 218, 108140.

[3] Antoni, J., & Randall, R. B. (2006). The spectral kurtosis: application to the vibratory surveillance and diagnostics of rotating machines. Mechanical systems and signal processing, 20(2), 308-331.

[4] Randall, R. B., Antoni, J., & Chobsaard, S. (2001). The relationship between spectral correlation and envelope analysis in the diagnostics of bearing faults and other cyclostationary machine signals. Mechanical systems and signal processing, 15(5), 945-962.

[5] Zheng, K., Li, T., Su, Z., Wen, J., Zhang, B., & Zhang, Y. (2019). Faults diagnosis of rolling bearings based on shift invariant K-singular value decomposition with sensitive atom nonlocal means enhancement. Measurement, 135, 836-851.

[6] Yan, X., Liu, Y., & Jia, M. (2019). Research on an enhanced scale morphological-hat product filtering in incipient fault detection of rolling element bearings. Measurement, 147, 106856.

[7] Lu, S., He, Q., & Wang, J. (2019). A review of stochastic resonance in rotating machine fault detection. Mechanical Systems and Signal Processing, 116, 230-260.

[8] Li, G., Tang, G., Wang, H., & Wang, Y. (2019). Blind source separation of composite bearing vibration signals with low-rank and sparse decomposition. Measurement, 145, 323-334.

[9] Wang, H., Ren, B., Song, L., & Cui, L. (2019). A novel weighted sparse representation classification strategy based on dictionary learning for rotating machinery. IEEE Transactions on Instrumentation and measurement, 69(3), 712-720.

[10] Had, A., & Sabri, K. (2019). A two-stage blind deconvolution strategy for bearing fault vibration signals. Mechanical Systems and Signal Processing, 134, 106307.

[11] Ou, L., Yu, D., & Yang, H. (2016). A new rolling bearing fault diagnosis method based on GFT impulse component extraction. Mechanical Systems and Signal Processing, 81, 162-182.

[12] del Rosario Bautista-Morales, M., & Patiño-López, L. D. (2023). Acoustic detection of bearing faults through fractional harmonics lock-in amplification. Mechanical Systems and Signal Processing, 185, 109740.

[13] Poik, M., Kohl, D., Mayr, M., Kerschner, C., & Schitter, G. (2020). A mechatronic lock-in amplifier: Integrating demodulation in sensor electronics for measuring mechanical oscillations. IEEE Transactions on Instrumentation and Measurement, 70, 1-8.

[14] Sonnaillon, M. O., & Bonetto, F. J. (2007). Lock-in amplifier error prediction and correction in frequency sweep measurements. Review of scientific instruments, 78(1).

[15] Chen, B., Zhang, W., Song, D., & Cheng, Y. (2020). Blind deconvolution assisted with periodicity detection techniques and its application to bearing fault feature enhancement. Measurement, 159, 107804.

[16] Stockham, T. G., Cannon, T. M., & Ingebretsen, R. B. (1975). Blind deconvolution through digital signal processing. Proceedings of the IEEE, 63(4), 678-692.

[17] Rai, A., & Upadhyay, S. H. (2016). A review on signal processing techniques utilized in the fault diagnosis of rolling element bearings. Tribology International, 96, 289-306.

[18] Lee, J. Y., & Nandi, A. K. (1998). Blind deconvolution of impacting signals using higher-order statistics. Mechanical systems and signal processing, 12(2), 357-371.

[19] Lee, J. Y., & Nandi, A. K. (2000). Extraction of impacting signals using blind deconvolution. Journal of Sound and Vibration, 232(5), 945-962.

[20] Wiggins, R. A. (1978). Minimum entropy deconvolution. Geoexploration, 16(1-2), 21-35.

[21] McDonald, G. L., Zhao, Q., & Zuo, M. J. (2012). Maximum correlated Kurtosis deconvolution and application on gear tooth chip fault detection. Mechanical Systems and Signal Processing, 33, 237-255.

[22] McDonald, G. L., & Zhao, Q. (2017). Multipoint optimal minimum entropy deconvolution and convolution fix: application to vibration fault detection. Mechanical Systems and Signal Processing, 82, 461-477.

[23] BIPM, IEC, IFCC, ILAC, ISO, IUPAC, IUPAP, and OIML. (2008). Evaluation of measurement data — Guide to the expression of uncertainty in measurement. Joint Committee for Guides in Metrology, JCGM 100:2008.

[24] BIPM, IEC, IFCC, ILAC, ISO, IUPAC, IUPAP, and OIML. (2008). Evaluation of measurement data — Supplement 1 to the "Guide to the expression of uncertainty in measurement" — Propagation of distributions using a Monte Carlo method. Joint Committee for Guides in Metrology, JCGM 101:2008.

[25] Cheng, Y., Zhou, N., Zhang, W., & Wang, Z. (2018). Application of an improved minimum entropy deconvolution method for railway rolling element bearing fault diagnosis. Journal of sound and vibration, 425, 53-69.

[26] Cheng, Y., Wang, Z., Zhang, W., & Huang, G. (2019). Particle swarm optimization algorithm to solve the deconvolution problem for rolling element bearing fault diagnosis. Isa Transactions, 90, 244-267.

[27] BIPM, IEC, IFCC, ILAC, ISO, IUPAC, IUPAP, and OIML. (2012). International vocabulary of metrology — Basic and general concepts and associated terms (VIM). Joint Committee for Guides in Metrology, JCGM 200:2012. (3rd edition).

[28] https://www.mfpt.org/fault-data-sets/